

## Ingeniería y Ciencia

Ingeniería y Ciencia

ISSN: 1794-9165

ingciencia@eafit.edu.co

Universidad EAFIT

Colombia

Fernández, M. E.; Murillo Y., G.; Vargas, R. A.; Peña Lara, D.; Diosa, J. E.  
Improvement of Proton-Exchange Membranes Based on (1-x) (H<sub>3</sub>PO<sub>2</sub>/PVA)-xTiO<sub>2</sub>  
Ingeniería y Ciencia, vol. 13, núm. 25, enero-junio, 2017, pp. 153-166  
Universidad EAFIT  
Medellín, Colombia

Available in: <http://www.redalyc.org/articulo.oa?id=83550861006>

- How to cite
- Complete issue
- More information about this article
- Journal's homepage in redalyc.org

redalyc.org

Scientific Information System

Network of Scientific Journals from Latin America, the Caribbean, Spain and Portugal

Non-profit academic project, developed under the open access initiative

# Improvement of Proton-Exchange Membranes Based on $(1 - x)(\text{H}_3\text{PO}_2/\text{PVA}) - x\text{TiO}_2$

M. E. Fernández <sup>1</sup>, G. Murillo Y. <sup>2</sup> R. A. Vargas <sup>3</sup>, D. Peña Lara <sup>4</sup> and J. E. Diosa <sup>5</sup>

Received: 27-11-2016 | Accepted: 25-04-2017 | Online: 08-05-2017

MSC: 82D60 | PACS: 72.80.Le, 72.80.Tm, 66.30.hk, 66.30.jp

doi:10.17230/ingciencia.13.25.6

---

## Abstract

Using impedance spectroscopy (IS), differential scanning calorimetry (DSC), thermogravimetric analysis (TGA), and infrared spectroscopy (IR) techniques to study the polymer electrolyte membranes based on poly(vinyl alcohol) (PVA) and hypophosphorous acid ( $\text{H}_3\text{PO}_2$ ) with different titanium oxide nanoparticles ( $\text{TiO}_2$ ) concentrations. The polymer systems  $(1-x)(\text{H}_3\text{PO}_2/\text{PVA}) + x\text{TiO}_2$  were prepared using the sol-casting method and different weight percent of  $\text{TiO}_2$ ,  $x \leq 10.0\%$ . The DSC results show that the glass transition for molar fraction  $\text{P}/\text{OH} = 0.3$  appears around

---

<sup>1</sup> Universidad del Valle, mariaferlo2000@yahoo.com,  
<http://orcid.org/0000-0003-4228-9693>, Cali, Colombia.

<sup>2</sup> Universidad Icesi, gustavo.murillo@correo.icesi.edu.co,  
<http://orcid.org/0000-0001-5172-4584>, Cali, Colombia.

<sup>3</sup> Universidad del Valle, ruben.vargas@correounivalle.edu.co,  
<http://orcid.org/0000-0002-2295-373X>, Cali, Colombia.

<sup>4</sup> Universidad del Valle, diego.pena@correounivalle.edu.co,  
<http://orcid.org/0000-0001-6199-1547>, Cali, Colombia.

<sup>5</sup> Universidad del Valle, jesus.diosa@correounivalle.edu.co,  
<http://orcid.org/0000-0002-1919-1922>, Cali, Colombia.

75°C and for the samples doped with  $\text{TiO}_2$  around 35°C; the melting point for all membranes appear around 175°C. The FTIR spectra show changes in the profiles of the absorption bands with the addition of  $\text{H}_3\text{PO}_2$  and the different concentrations of  $\text{TiO}_2$ . The IS results show dielectric and conductivity relaxations as well as a change in DC ionic conductivity with the  $\text{TiO}_2$  content. The order of the ionic conductivity is about  $10^{-2}$  S/cm for 5.0% of  $\text{TiO}_2$ . The TGA in the heating run shows water loss that is in agreement with DC conductivity measurements.

**Key words:** Composite polymer membranes; PVA; Hypophosphorous acid; Proton conduction, DC conductivity.

---

## Mejoras en membranas de intercambio protónico $(1-x)(\text{H}_3\text{PO}_2/\text{PVA})-x\text{TiO}_2$

---

### Resumen

Usando las técnicas de espectroscopia de impedancia (IS), calorimetría de barrido diferencial (DSC), análisis termogravimétrico (TGA) y espectroscopia infrarroja (FTIR) se estudió el sistema polimérico  $(1-x)(\text{H}_3\text{PO}_2/\text{PVA}) + x\text{TiO}_2$  el cual fue preparado usando el método de *sol-casting* a diferentes porcentaje de peso de nanopartículas de  $\text{TiO}_2$ ,  $x \leq 10.0\%$ . Los resultados de DSC muestran que la transición vítrea para la fracción molar de  $\text{P}/\text{OH} = 0.3$  emerge alrededor de 75°C y para las muestras dopadas con  $\text{TiO}_2$  alrededor de 35°C; el punto de fusión para todas las membranas aparece alrededor de los 175°C. Los espectros de FTIR muestran cambios en los perfiles de las bandas de absorción con la adición del  $\text{H}_3\text{PO}_2$  y las diferentes concentraciones de  $\text{TiO}_2$ . Los resultados de IS muestran relajaciones dieléctricas y de conductividad al igual que un cambio en la conductividad iónica DC con el contenido de  $\text{TiO}_2$ . La conductividad iónica es del orden de  $10^{-2}$  S/cm para 5.0% de  $\text{TiO}_2$ . Los TGA en los barridos de calentamiento muestran pérdida de agua lo cual está de acuerdo con las medidas de conductividad DC.

**Palabras clave:** Membranas poliméricas compositos; PVA; conducción protónica.

---

## 1 introduction

The Proton Exchange Membranes (PEMs) are the most promising for Fuel Cells (FC) technologies to generate clean energy [1],[2],[3],[4]. Perfluorinated Nafion<sup>®</sup> is the most used membrane for FC applications [5],[6],

due to excellent chemical stability and a marked effect on the proton conductivity. A more economical alternative for preparing PEM was proposed in 1989 [7] which is a combination of poly(vinyl alcohol) (PVA) and hypophosphorous acid. This new combination allowed the production of non-perfluorinated membranes of low cost and good procesability, encouraging manufacturing different types of PEMs, which have been synthesized using mixtures of polymers with various salts and acids [8]. Other groups have investigated various combinations using PVA as polymeric matrix [8],[9],[10],[11],[12]. On the other hand, composites have been synthesized based on polymeric membranes combined with micro or nanoparticles for the purpose of controlling the physical and chemical properties, being in some cases that this approach has improved proton conductivity and mechanical properties for some dispersant concentrations [13],[14],[15],[16]. In this work the polymer membrane ( $\text{H}_3\text{PO}_2/\text{PVA}$ ) with constant molar ratio  $\text{P}/\text{OH} = 0.3$ , doped with  $\text{TiO}_2$  nanoparticles have been synthesized and studied its effect on the thermal and electrical properties.

## 2 Experimental methods

The precursors materials were hypophosphorous acid ( $\text{H}_3\text{PO}_2$ ), PVA, and titanium oxide ( $\text{TiO}_2$ ) with particle size smaller than 50 nm (Sigma Aldrich Chemicals). PVA was poured in distilled water at  $90^\circ\text{C}$  using a magnetic stirrer plate to completely dissolve the polymer. After turning off the stirrer, constant amounts of acid were added to the solution, according to the molar ratio  $\text{P}/\text{OH} = 0.3$ . Then, constant amounts of  $\text{TiO}_2$  nanoparticles were added to the solution, maintaining the mixture under agitation until it became homogeneous. After additional two hours under agitation the mixture, now at room temperature, was poured into glass vessels under dry atmosphere (desiccator with sulphuric acid) by several days to obtain membranes. The resulting membranes were uniform, smooth, homogeneous with a constant white color on the whole surface due to the presence of highly dispersed  $\text{TiO}_2$  nanoparticles, and having a thickness of 0.2 mm.

The thermal characterization was carried out by using a TA Instrument DSC Q100 calorimeter at a thermal scan of  $10^\circ\text{C}/\text{min}$  under a nitrogen atmosphere in a temperature range between  $-75^\circ\text{C}$  and  $250^\circ\text{C}$ . Thermogravimetric characterization (TG) was carried out with a TA instruments 2050

TGA microbalance at a temperature rate of  $10^\circ\text{C}/\text{min}$  under a nitrogen atmosphere from ambient temperature to  $180^\circ\text{C}$ .

The electrical characterizations of the samples were performed by impedance spectroscopy (IS) using an Agilent 4294A impedance analyzer in a frequency range 40 Hz to 6 MHz, with a voltage signal of 500 mV peak-to-peak. The measurements were done at isotherms separated by  $10^\circ\text{C}$  between room temperature and  $120^\circ\text{C}$ , under an air atmosphere. Cylindrical silver electrodes of 5.0 mm in diameter were used to contact the samples. The dc conductivity was determined from the bulk sample resistance using the impedance plots,  $Z$ , by extrapolation of the circular portion of the spectrum to the real axis  $Z'$ , and then using the expression  $\sigma_0 = d/AR$  being  $R$  the intercept with the  $Z'$ -axis,  $d$  the membrane thickness, and  $A$  the sample contact area with the electrodes. The Jonscher model [17]

$$\sigma(\omega) = \sigma_0 + A\omega^n \quad (1)$$

was used to determine  $\sigma_0$  by fitting experimental data, where  $\sigma_0$  is the dc conductivity (independent of frequency),  $A$  is a pre-exponential factor related to crossover frequency,  $\omega_p$ , and  $n$  is between 0 and 1.

From the impedance data,  $Z'(\omega)$  and  $Z''(\omega)$ , the values for real part of the conductivity ( $\sigma'$ ), real part ( $\epsilon'$ ), and imaginary part ( $\epsilon''$ ) of the permittivity were obtained by following relations:

$$\sigma'(\omega) = \frac{Z''}{Z'^2 + Z''^2} \quad (2)$$

$$\epsilon' = \frac{Z''}{\omega C_0(Z'^2 + Z''^2)} \quad (3)$$

$$\epsilon'' = \frac{Z'}{\omega C_0(Z'^2 + Z''^2)} \quad (4)$$

where  $C_0$  is the empty cell capacitance.

The Fourier transform infrared spectra, FT-IR, were recorded using a Vertex 70 with resolution  $4\text{ cm}^{-1}$ , on an interval from  $4000\text{ cm}^{-1}$  to  $500\text{ cm}^{-1}$ . Spectra were obtained at room temperature and under a nitrogen atmosphere.

### 3 Result and discussions

Typical DSC curves for  $(1 - x)(\text{H}_3\text{PO}_2/\text{PVA}) - x\text{TiO}_2$  membranes with constant ratio  $\text{P}/\text{OH} = 0.3$  and different concentrations  $x$  (for 0.0%, red; 2.5%, green; 5.0%, blue; 7.5%, navy; 10.0%, olive) of  $\text{TiO}_2$  are depicted in Figure 1.

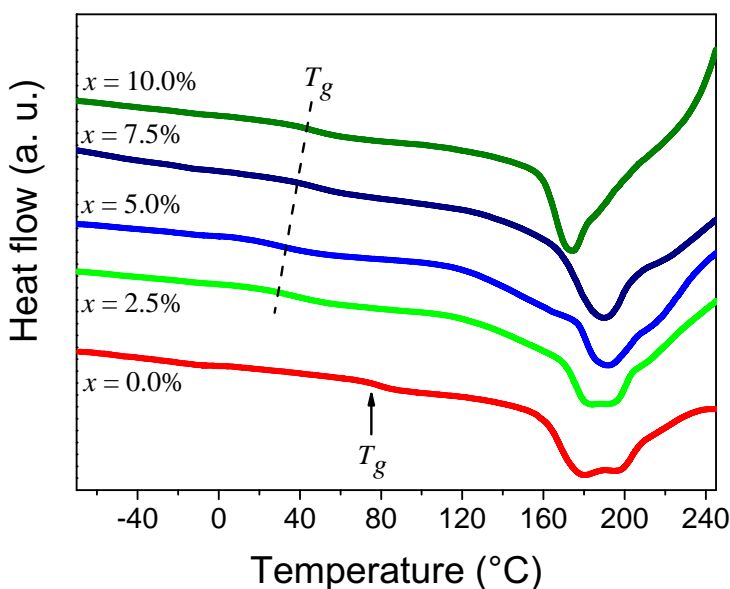


**Figure 1:** DSC curves for the  $(1 - x)(\text{H}_3\text{PO}_2/\text{PVA}) - x\text{TiO}_2$  membranes with  $\text{TiO}_2$  content of  $x = 0.0\%$  (red),  $2.5\%$  (green),  $5.0\%$  (blue),  $7.5\%$  (navy), and  $10.0\%$  (olive), from  $-75^\circ\text{C}$  to  $250^\circ\text{C}$  using a heating rate of  $10^\circ\text{C}/\text{min}$  under a dry  $\text{N}_2$  flux. The vertical arrow (for  $x = 0.0\%$ ) and the dotted line (for  $x = 2.5\%$ ,  $5.0\%$ ,  $7.5\%$ , and  $10.0\%$ ) indicate  $T_g$ .

It was reported [8] previously, for  $\text{H}_3\text{PO}_2$  and PVA based membranes with acid high concentrations and high degree of hydration of the polymer that the glass transition temperature ( $T_g$ ) was below  $0.0^\circ\text{C}$ . In our case, for low acid concentrations ( $\text{P}/\text{OH} = 0.3$ ,  $x = 0.0\%$ ) the  $T_g$  is around  $75^\circ\text{C}$  (as indicated by the vertical arrow) while for  $\text{TiO}_2$  doped samples the  $T_g$

appears around  $35^\circ\text{C}$  (as indicated by a dotted line), thus clearly indicating the effect of the oxide filler. The melting point for all membranes is observed at around  $175^\circ\text{C}$ .

FT-IR spectra for PVA and  $(1 - x)(\text{H}_3\text{PO}_2/\text{PVA})\text{-}x\text{TiO}_2$  system are showed in Figure 2.

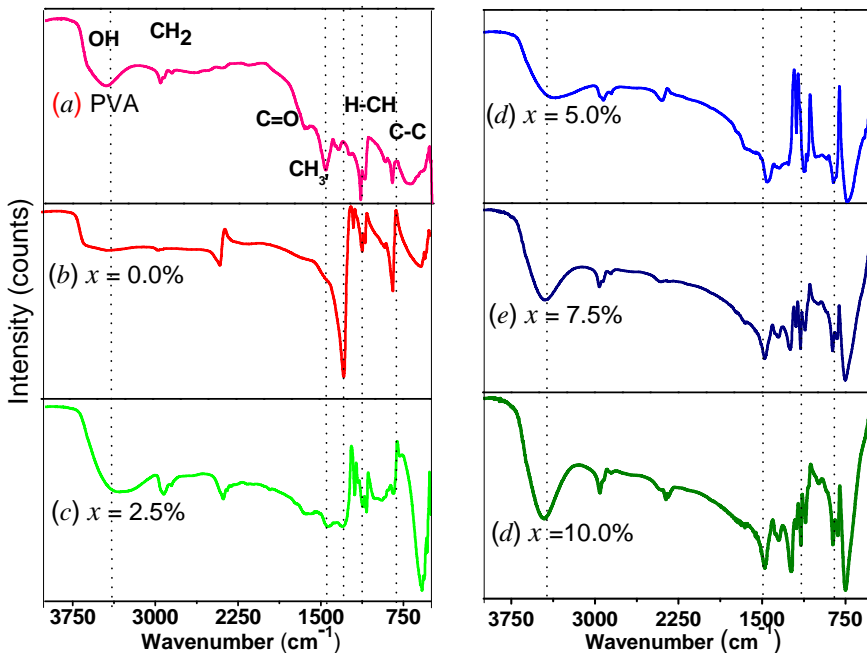


**Figure 2:** FT-IR spectra of PVA and  $(1 - x)(\text{H}_3\text{PO}_2/\text{PVA})\text{-}x\text{TiO}_2$  with  $\text{TiO}_2$  content of  $x = 0.0\%$  (red),  $2.5\%$  (green),  $5.0\%$  (blue),  $7.5\%$  (navy), and  $10.0\%$  (olive).

For pure PVA, four characteristic absorption bands are observed: the one at  $3485\text{ cm}^{-1}$  which is assigned to vibration along the C–OH-chains bonds in PVA; the second one at  $2957\text{ cm}^{-1}$  attributed to asymmetric elongation of the CH–CH<sub>2</sub>-groups. The third one at  $1477\text{ cm}^{-1}$  was associated with CH-cross deformations in CH<sub>2</sub>-groups and the fourth band at  $742\text{ cm}^{-1}$  was assigned to H–C–C–H-bound modes in the CH<sub>2</sub> groups. Additionally, the  $\text{H}_3\text{PO}_2/\text{PVA}$  system was also characterized. In this case, two

additional bands appeared which were associated with vibration along the  $V_{as}(PO_2)$ -antisymmetric bonds and the  $V_s(PO_2)$ -symmetric bonds at  $1269\text{ cm}^{-1}$  and  $1102\text{ cm}^{-1}$ , respectively. Finally, by the addition of different  $TiO_2$  concentrations, spectra show changes (movement and intensification of the peaks) for bands associated to  $CH_3$ ,  $PO_2$ ,  $CH_2$ , and C–C functional groups. These changes might be related to effects of approximation of the nanoparticles with the polymer chains.

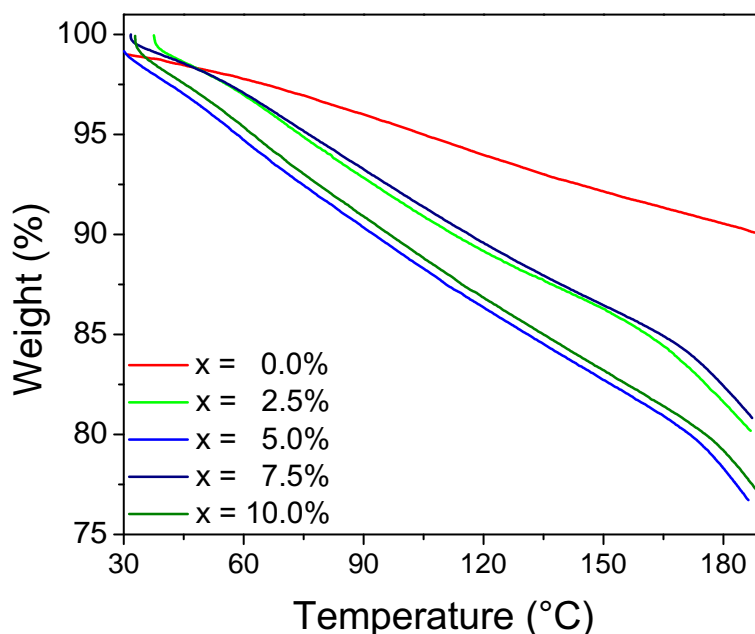


**Figure 3:** TGA curves of  $(1 - x)(H_3PO_2/PVA) - xTiO_2$  with  $TiO_2$  content of  $x = 0.0\%$  (red),  $2.5\%$  (green),  $5.0\%$  (blue),  $7.5\%$  (navy), and  $10.0\%$  (olive).

Figure 3 shows the TGA curves of the membranes at a heating rate of  $10^{\circ}C/min$ . It is observed that all the TGA curves show a continuous weight loss as the temperature is increased. This loss is attributable to the evaporation of water molecules absorbed on the membrane surface or trapped within the chains of the polymer matrix. However, it is important to note that the losses presented between room temperature and  $100^{\circ}C$  increases with the concentration of  $TiO_2$  indicating higher water content



in the fresh samples as the oxide filler content increases. Later on, the electrical measurements will reflect the influence of water removal from the samples on their proton conductivities.

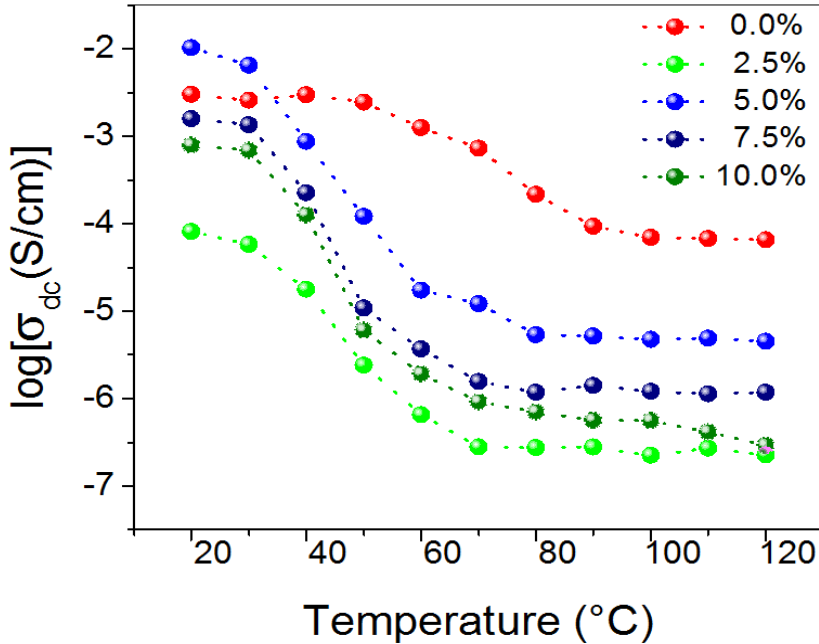


**Figure 4:** Temperature variation of the dc conductivity of  $(1-x)(\text{H}_3\text{PO}_2/\text{PVA})-x\text{TiO}_2$  with  $\text{TiO}_2$  content of  $x = 0.0\%$  (red),  $2.5\%$  (green),  $5.0\%$  (blue),  $7.5\%$  (navy), and  $10.0\%$  (olive).

Figure 4 shows the temperature variation of dc conductivity on a logarithm scale calculated from the impedance Nyquist plots of the  $(1-x)(\text{H}_3\text{PO}_2/\text{PVA})-x\text{TiO}_2$  membrane. The results show that dc conductivity values decrease with increasing temperature in the range where the membranes release water as noted in the results of TGA (see Figure 3) indicating that the proton transport membranes is provided in regions containing water that form a liquid phase or aqueous solution with  $\text{H}_3\text{PO}_2$ . This liquid phase coexists with a solid phase of the reinforced polymer, consisting of PVA, the acid which is not dissolved in the liquid phase, and the dispersed  $\text{TiO}_2$  particles, as discussed in references [9] and [18] for similar

polymeric membranes. This phenomenon is common in perfluorinated hydrated membranes (Nafion<sup>®</sup>). The dc conductivity is between  $10^{-5}$  S/cm to  $10^{-2}$  S/cm at room temperature, being about  $10^{-2}$  S/cm for 5.0% TiO<sub>2</sub>. Furthermore, above a decreasing step of dc conductivity, it remains at a constant value with increasing temperatures for each concentration. Conductivity values in this high-temperature interval have values from  $10^{-6}$  S/cm to  $10^{-4}$  S/cm that depends on concentration and the highest one correspond to  $x = 0.0\%$ .

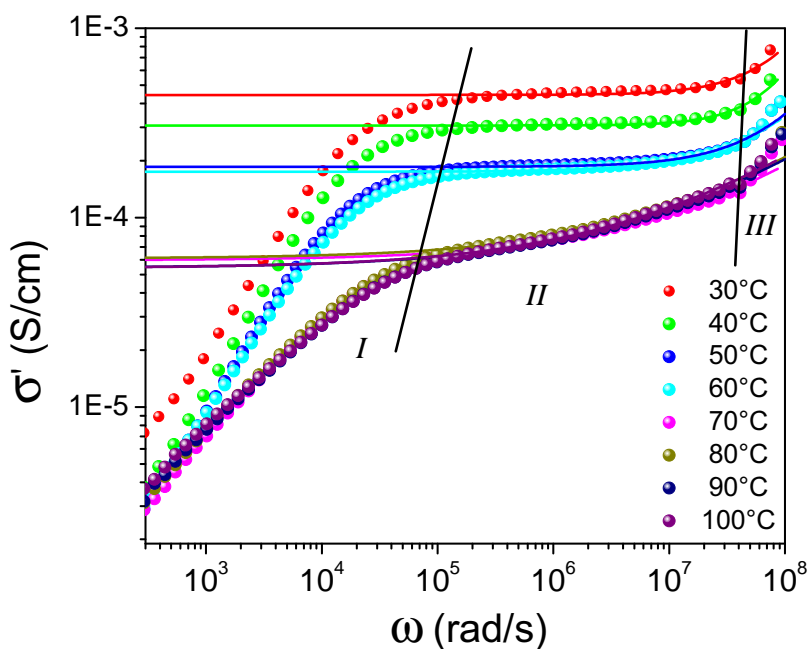


**Figure 5:** Log-log plot of the real part of the conductivity ( $\sigma'$ ) as a function of (angular) frequency ( $\omega$ ) for  $(1-x)$  ( $\text{H}_3\text{PO}_2/\text{PVA}$ )- $x\text{TiO}_2$  with  $\text{TiO}_2$  content of  $x = 10.0\%$  at several isotherms at  $30^\circ\text{C}$  (red),  $40^\circ\text{C}$  (green),  $50^\circ\text{C}$  (blue),  $60^\circ\text{C}$  (cyan),  $70^\circ\text{C}$  (magenta),  $80^\circ\text{C}$  (dark yellow),  $90^\circ\text{C}$  (navy), and  $100^\circ\text{C}$  (purple). Solid line represents a Jonscher model fitting according to Equation (1).

Figure 5 shows the real part of the electrical conductivity  $\sigma'$  as a function of the (angular) frequency [ $\omega = 2\pi f$  (Hz)] in double logarithmic scale at different isotherms. In all spectra it can be seen three distinct regions

as the temperature increases: at low frequency, a strongly dispersive initial region (*I*) which corresponds to the charge transfer processes at the electrode-electrolyte interface, followed by an intermediate less dispersive frequency region (*II*) corresponding to the long range ionic transport (dc-regime). Notice that  $\sigma'$  decreases with increasing temperature between 20°C and 120°C. Finally, a highly dispersive frequency region (*III*), in which the conductivity increases rapidly with increasing frequency. This phenomenology can be attributed to strong correlations in the hopping of charge carriers (relaxation of conductivity). The behavior in region *II* and *III* follow the power law proposed by Jonscher [17],  $\sigma'(\omega) = \sigma_0 + A\omega^n$ , where  $n$  is a fractional exponent between 0 and 1. The parameter  $n$  has been proposed to be close to 1 for strongly correlated ion motion and to be equal to zero for completely random and independent Debye-like ion hops [17]. The Jonscher phenomenological model was used to fit the experimental data of the conductivity  $\sigma'$  as a function of frequency represented by a solid line in Figure 5 to obtain  $\sigma_0$ ,  $n$ , and  $\omega_p$  parameters.

**Table 1:** Fitting parameters obtained from the Jonscher model for membrane with concentration  $x = 10.0\%$ .

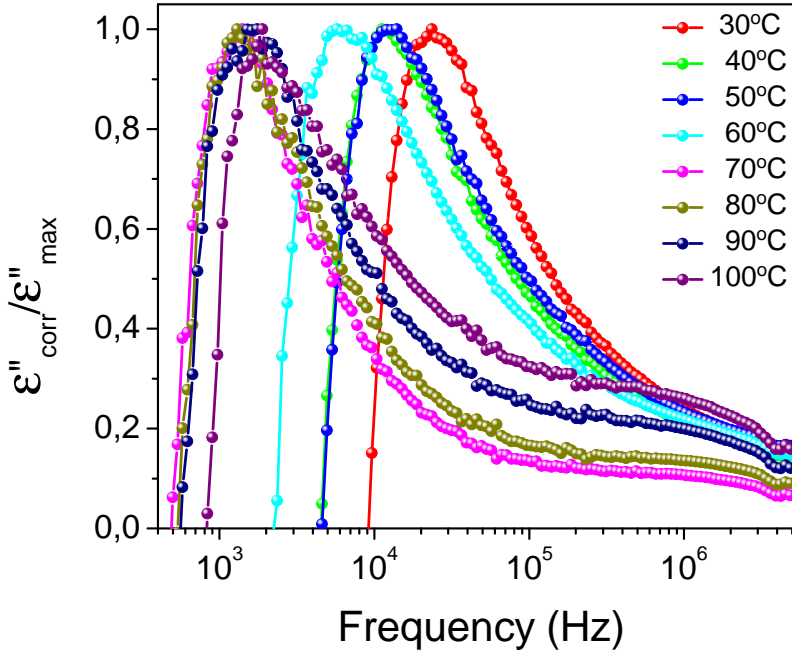
$T$ (°C)	$n$	$A$	$\sigma_0$ (S/cm)
30	1.23	$4.620 \times 10^{-14}$	$4.44 \times 10^{-4}$
40	1.44	$8.298 \times 10^{-16}$	$3.06 \times 10^{-4}$
50	1.00	$1.253 \times 10^{-12}$	$1.85 \times 10^{-4}$
60	0.86	$2.048 \times 10^{-11}$	$1.74 \times 10^{-4}$
70	0.46	$2.939 \times 10^{-8}$	$5.95 \times 10^{-5}$
80	0.44	$4.134 \times 10^{-8}$	$6.08 \times 10^{-5}$
90	0.43	$5.879 \times 10^{-8}$	$5.43 \times 10^{-5}$
100	0.42	$6.411 \times 10^{-8}$	$5.42 \times 10^{-5}$

Table 1 gives the values for  $n$ ,  $A$ , and  $\sigma_0$  according to Jonscher model for the membrane with  $x = 10.0\%$ . It is important to stress that the dc conductivity ( $\sigma_0$ ) values coincide those calculated from Nyquist plots. On the other hand, the  $n$ -exponent parameters are between 0 and 1, except data recorded at 30°C and 40°C which give values higher than 1 that may be associated with high values of energy storage in the collective movements of the short-range ions and which can not be explained by Jonscher

model. Moreover, the crossover frequency ( $\omega_p$ ) values decrease with increasing temperature similar to those of dc conductivity. This observation indicates that all processes of ion transport, either long-range (dc conductivity) or relaxation (characterized by the frequency  $\omega_p$ ), have the same origin, that is, migration (jump) of the charge carriers in the polymeric matrix.

In terms of the dielectric permittivity, calculated from equation (3) and (4) for its real and imaginary parts, we have:

$$\varepsilon(\omega) = \varepsilon'(\omega) - i\varepsilon''(\omega) \quad (5)$$



**Figure 6:** The correct and normalized imaginary part of dielectric permittivity,  $\varepsilon''_{\text{corr}}/\varepsilon''_{\text{max}}$ , for the  $(1-x)(\text{H}_3\text{PO}_2/\text{PVA})-x\text{TiO}_2$  membrane with  $\text{TiO}_2$  content of  $x = 10.0\%$  at different isotherms as a function of frequency in logarithm scale. The solid lines are guides to the eye.

Figure 6 shows the result for the corrected and normalized imaginary part of dielectric permittivity,  $\varepsilon''_{\text{corr}}/\varepsilon''_{\text{max}}$ , where  $\varepsilon''_{\text{corr}} = \varepsilon'' - \sigma_0/w$  for the

composite concentration  $x = 10.0\%$ . Here we observe a dielectric relaxation peak at low temperature and relatively low frequency. This peak is observed at around  $10^3$  Hz at different isotherms. We attribute this relaxation to the presence of water in the polymer that introduce polar effect in the composite.

## 4 Conclusions

Composite polymer electrolyte based on PVA- $\text{H}_3\text{PO}_2$ , with constant molar ratio  $\text{P}/\text{OH} = 0.3$ , and reinforced with nanoparticles  $\text{TiO}_2$  (doping concentration  $x \leq 10.0\%$ ), homogenously dispersed, have been prepared. The TGA results show that the oxide filler of  $\text{TiO}_2$  nanoparticles increases the water content in the hydrated composites. Moreover, the DSC results show that the glass transition for membranes based on  $\text{H}_3\text{PO}_2$  and PVA with high acid concentrations and high degree of hydration of PVA is below  $0^\circ\text{C}$ , as reported previously, which is shifted to about  $75^\circ\text{C}$  for membranes with a low acid concentration of  $\text{P}/\text{OH} = 0.3$ , thus indicating that the acid aqueous solution plasticizes the polymer. However, when the membranes are reinforced with  $\text{TiO}_2$  the glass transition temperature decrease to  $35^\circ\text{C}$ , thus suggesting that the water content increases due to the presence of the porous  $\text{TiO}_2$  nanoparticles which increases the plasticity of the blends. On the other hand, the melting point appears at around  $175^\circ\text{C}$  for all membranes, close to that of the polymer matrix of PVA, indicating identical bond strength. Infrared spectroscopy spectra for pure PVA, as well as with acid content and with dispersed  $\text{TiO}_2$  nanoparticles show variation in the absorption peaks indicating that the acid and  $\text{TiO}_2$  are chemically coordinated to the PVA chains.

DC conductivity is in the range  $10^{-5}$  S/cm to  $10^{-2}$  S/cm at room temperature for  $\text{TiO}_2$  concentrations examined, reaching its maximum value of  $10^{-2}$  S/cm for a 5.0%- $\text{TiO}_2$  concentration.

The real part of the conductivity as a function of frequency shows a behavior known as Jonscher's power-law, with a crossover frequency ( $\omega_p$ ) associated with relaxation in the mobile ions. The temperature-dependency of  $\omega_p$  follows the temperature variation of the dc conductivity, suggesting a common origin in these processes as a consequence of correlations among ions hopping.

The permittivity of the hydrated samples (at lower temperatures) shows as a function of frequency dielectric relaxation peaks in its imaginary part that we attribute to the polar effect of the water molecule in the membranes.

## Acknowledgments

Financial support by Excellence Center for Novel Materials (CENM) is gratefully acknowledged.

## References

- [1] B. Smitha, S. Sridhar, and A. Khan, "Solid polymer electrolyte membranes for fuel cell applications –a review," *J. Membrane Science*, vol. 259, pp. 10–26, 2005. 154
- [2] J. Rao and K. Geckeler, "Polymer nanoparticles: Preparation techniques and size-control parameters," *Progress in Polymer Science*, vol. 48, pp. 887–913, 2003. 154
- [3] H. Zhang and S. P. Kang, "Recent Development of Polymer Electrolyte Membranes for Fuel Cells," *Chem. Rev.*, vol. 112, pp. 2780–2832, 2012. 154
- [4] A. Mazuera and R. Vargas, "Electrical Properties and Phase Behavior of Proton Conducting Nanocomposites Based on the Polymer System  $(1-x)[\text{PVOH} + \text{H}_3\text{PO}_2 + \text{H}_2\text{O}]\hat{\text{A}}\cdot x(\text{Nb}_2\text{O}_5)$ ," *Am. J. Analytical Chem.*, vol. 5, pp. 301–307, 2014. 154
- [5] J. B. Goodenough, "Proton conductors: Solids, membranes, and gels—materials and devices. edited by phillippe colomban, cambridge university press, cambridge, uk 1992, £ 75, xxxii, 581 pp., hardcover, isbn 0-521-38317-x," *Advanced Materials*, vol. 5, no. 9, pp. 683–685, 1993. [Online]. Available: <http://dx.doi.org/10.1002/adma.19930050923> 154
- [6] S. Banerjee and D. Curtin, "Nafion<sup>®</sup> perfluorinated membranes in fuel cells," *J. Fluorine Chem.*, vol. 125, pp. 1211–1216, 2004. 154
- [7] K. Gong and H. Shou-Cai, "Electrical Properties of Poly(Vinyl Alcohol) Complexed with Phosphoric Acid," *Mater. Res. Soc. Symp. Proc.*, vol. 135, pp. 377–382, 1989. 155
- [8] M. Vargas, R. Vargas, and B.-E. Mellander, "More studies on the PVAI+  $\text{H}_3\text{PO}_2 + \text{H}_2\text{O}$  proton conductor gels," *Electrochimical Acta*, vol. 45, pp. 1399–1403, 2000. 155, 157

- [9] I. Palacio, R. Castillo, and R. Vargas, "Thermal and transport properties of the polymer electrolyte based on poly (vinyl alcohol) –KOH–H<sub>2</sub>O," *Electrochemical Acta*, vol. 48, pp. 2195–2199, 2003. 155, 160
- [10] V. Zapata, W. Castro, R. Vargas, and B.-E. Mellander, "More studies on the PVOH–LiH<sub>2</sub>PO<sub>4</sub> polymer system," *Electrochimical Acta*, vol. 53, pp. 1476–1480, 2007. 155
- [11] W. Castro, V. Zapata, R. Vargas, and B.-E. Mellander, "Electrical conductivity relaxation in PVOH–LiClO<sub>4</sub>–Al<sub>2</sub>O<sub>3</sub>," *Electrochimica Acta*, vol. 53, pp. 1422–1426, 2007. 155
- [12] M. Fernández, J. Castillo, F. Bedoya, J. Diosa, and R. Vargas, "Dependence of the mechanical and electrical properties on the acid content in PVA + H<sub>3</sub>PO<sub>2</sub> + H<sub>2</sub>O membranes," *Rev. Mex. Física*, vol. 60, pp. 249–252, 2014. 155
- [13] C. Yang, "Synthesis and characterization of the cross-linked PVA/TiO<sub>2</sub> composite polymer membrane for alkaline DMFC," *Electrochimical Acta*, vol. 288, pp. 51–60, 2007. 155
- [14] M. Fernández, J. Diosa, R. Vargas, J. Guerra, C. Villaquiran, D. García, and J. Eiras, "Influence of TiO<sub>2</sub> Nanoparticles on the Morphological, Thermal and Solution Properties of PVA/TiO<sub>2</sub> Nanocomposite Membranes," *Phys. Stat. Sol. (c)*, vol. 4, pp. 4075–4080, 2007. 155
- [15] P. Ahmadpoor, A. Nateri, and V. Motaghitalab, "The Optical Properties of PVA/TiO<sub>2</sub> Composite Nanofibers," *J. Applied Polymer Science*, vol. 130, pp. 78–85, 2013. 155
- [16] J. Ahmad, K. Deshmukh, M. Habib, and M. Hägg, "Influence of TiO<sub>2</sub> Nanoparticles on the Morphological, Thermal and Solution Properties of PVA/TiO<sub>2</sub> Nanocomposite Membranes," *J. Sci. Eng.*, vol. 39, pp. 6805–6814, 2014. 155
- [17] A. Jonscher, *Universal relaxation law: a sequel to Dielectric relaxation in solids*. Chelsea Dielectrics Press, 1996. 156, 162
- [18] G. Casalbore-Miceli, M. Yang, M. Camaioni, C.-M. Mari, Y. Li, M. Sun, and H. Ling, "Investigations on the ion transport mechanism in conducting polymer films," *Sol. Stat. Ionics*, vol. 131, pp. 6805–6814, 2000. 160